

Article

# Digitalizing Structure–Symmetry Relations at the Formation of Endofullerenes in Terms of Information Entropy Formalism

Denis Sh. Sabirov , Alina A. Tukhbatullina  and Igor S. Shepelevich

Laboratory of Mathematical Chemistry, Institute of Petrochemistry and Catalysis UFRC RAS, 450075 Ufa, Russia  
\* Correspondence: diozno@mail.ru; Tel.: +7-347-284-27-50

**Abstract:** Information entropy indices are widely used for numerical descriptions of chemical structures, though their applications to the processes are scarce. We have applied our original information entropy approach to filling fullerenes with a guest atom. The approach takes into account both the topology and geometry of the fullerene structures. We have studied all possible types of such fillings and found that information entropy ( $\Delta h_R$ ) and symmetry changes correlate.  $\Delta h_R$  is negative, positive or zero if symmetry is increased, reduced or does not change, respectively. The  $\Delta h_R$  value and structural reorganization entropy, a contribution to  $\Delta h_R$ , are efficient parameters for the digital classification of the fullerenes involved into the filling process. Based on the calculated values, we have shown that, as the symmetry of the fullerene cage becomes higher, the structural changes due to the filling it with a guest atom become larger. The corresponding analytical expressions and numerical data are discussed.

**Keywords:** information entropy; symmetry; topology–geometric relations; Jahn–Teller effect; fullerenes; endofullerenes; classification algorithm



**Citation:** Sabirov, D.S.; Tukhbatullina, A.A.; Shepelevich, I.S. Digitalizing Structure–Symmetry Relations at the Formation of Endofullerenes in Terms of Information Entropy Formalism. *Symmetry* **2022**, *14*, 1800. <https://doi.org/10.3390/sym14091800>

Academic Editor: Susmit Bagchi

Received: 30 June 2022

Accepted: 25 August 2022

Published: 30 August 2022

**Publisher's Note:** MDPI stays neutral with regard to jurisdictional claims in published maps and institutional affiliations.



**Copyright:** © 2022 by the authors. Licensee MDPI, Basel, Switzerland. This article is an open access article distributed under the terms and conditions of the Creative Commons Attribution (CC BY) license (<https://creativecommons.org/licenses/by/4.0/>).

## 1. Introduction

Information entropy (or Shannon entropy) and related quantities are widely used in structural and mathematical chemistry for numerically assessing the complexity of chemical objects [1–12]. One of the most common approaches deduces information entropy values from molecular graphs by counting atom types and their populations [13,14]. It treats a molecule as a system of subsets (atom types), whose number corresponds to the number of the signals in NMR spectra [14,15]. As previously found [13,15–17], such a partition of the fullerenes correlates with their symmetry point groups within a certain series of related or isomeric compounds. As the symmetry point group of the molecule becomes higher, its information entropy becomes lower, as was exemplified with the fullerene isomeric series of  $C_{60}$  [16] and  $C_{84}$  [15]. Moreover, information entropies of oligomers  $(C_{60})_n$  congruently oscillate with the rotational symmetry numbers depending on the odd/even number of a homolog in the series [18]. Correlations between the symmetry and information entropy could be also found in the case of crystalline compounds [12,19].

In general, the information entropy characterizes the complexity of the molecules more accurately than symmetry [8,20]. Importantly, these estimates may relate to physicochemical processes [7,21–24] and, therefore, may be applicable to searching for correlations between the molecular structure, macroscopic properties, activities, performances, etc. [4,5,8,11–13,15–17,25–29].

The inner cavity, as an empty space which can be filled with guest atoms, is one of the attractive features of fullerenes [30,31]. The atoms can be trapped by the fullerene cages during fullerene synthesis [32], or high-pressure/high-temperature techniques can be used to introduce guest species inside the yet synthesized fullerenes [33]. In the last case, the

formal chemical reaction occurs ( $X$  is a guest atom and  $N$  denotes the number of carbon atoms in the fullerene cage that is filled):



Such filling leads to changes in molecular/physicochemical properties and reactivity (e.g., [30,34–41]) and is accompanied with the slight extending of the fullerene cage [35,39] (with rare exceptions when the fullerene cage becomes more compact [42,43]). These changes have been scrutinized both theoretically and experimentally, and such studies usually include background discussions on the symmetry of the formed endofullerenes. However, their symmetry has never been addressed in a separate study. Encouraged by our recent advances in numerical descriptions of exohedral fullerene compounds with information entropy [13,17,18], we have decided to fill this gap.

In the present work, we consider typical cases of the formation of endofullerenes with single atoms inside in the aspect of the symmetry changes. For this purpose, we apply our original information-entropy-based formalism to the analysis of chemical processes [44]. Note that we do not look for correlations between the structural descriptors and the observed physicochemical properties. We instead focus on the interpretation of information entropy values in the context of digitalizing structural chemistry.

## 2. Preliminary Remarks

### 2.1. Mathematical Description of Fullerene Molecules

Fullerenes are very attractive models for structural chemistry studies, as their molecules are constructed in line with strict mathematical regularities. The topology of fullerenes has been discussed in a book [45] and in a comprehensive review [46], so here we make some important remarks on the relations between the topology, geometry and symmetry of the molecules.

Fullerenes are molecular objects, and their topology can be represented as molecular graphs [45,46]. The last ones in fullerene science are called Schlegel diagrams, which are introduced as the plain projections of polyhedra representing fullerene molecules (see examples in Section 4.5). Analyzing the corresponding adjacency matrices allows for the sortation of vertices over inequivalent types. For this purpose, the paths between the vertices are analyzed, and vertices are distributed over the topological orbits [45,46]. The exhaustive description of this topological approach can be also found in our studies [15,18].

There are algorithms connecting the topological parameters of Schlegel diagrams [45,46] with the expected symmetries of the fullerene molecules. Deduced from the topology, the symmetry of a certain fullerene corresponds to the highest one possible for this topological structure. In most cases, this ideal symmetry coincides with the actual one found on the level where geometry (spatial arrangement of atoms) is considered. However, on this level, reductions in symmetry can take place due to the Jahn–Teller effect (we scrutinize this case in Section 4.4). This reduction makes topologically equivalent atoms spatially inequivalent. To account for this geometrical inequivalence, one must perform a separate study of the symmetry based on the Cartesian coordinates of the atoms that make up the molecule. The coordinates for this purpose are usually obtained from high-level quantum chemical computations (e.g., [16,47]).

In brief, the symmetry of a fullerene molecule is deducible from its topology. However, it is better analyzed with the geometry of the molecule in order not to miss possible Jahn–Teller symmetry reduction. Herein, the topologies of the fullerene molecule in the high-symmetry and reduced-symmetry states are identical.

### 2.2. Information Entropy Formalism Applied to (Endo)Fullerenes

To apply information entropy formalism, the molecule must be presented as the set of the elements, atoms or bonds. We prefer to deal with representing molecules as sets of atoms due to two reasons [7]. First, the distribution of the molecule's atoms over atom types corresponds to its NMR spectrum, i.e., there is a direct correspondence to experimental

techniques. The second reason deals with a particular case of the chemical structure of endofullerenes. The atom placed inside has no covalent bonds with the fullerene cage. Hence, the molecular graph of endofullerene contains one isolated vertex, and considering the edges of this structure seems impractical.

Therefore, we treat (endo)fullerenes as sets of atoms which are distributed over atom types based on their geometries obtained in previous studies.

### 2.3. Topological Stability of the Fullerene Cages in Endofullerenes

Another note on endofullerenes deals with chemical aspects of their formation. When formed, the topology of the fullerene cage does not change. This regularity is rarely violated, and the corresponding cases are far from the objects under the present study, as they deal with further chemical transformations of the already formed endohedral complexes (e.g., the compression of endofullerenes with reactive fillings [38,48,49], the chemical reactions of metal carbide endofullerenes [50] and cage-opened fullerene derivatives [51]).

## 3. Computational Details

### 3.1. Information Entropy Indices for the Analysis of Chemical Processes

The fullerene molecules are represented as the sets of  $N_1$  atoms of the 1st type,  $N_2$  atoms of the 2nd type, . . . and  $N_n$  atoms of the  $n$ -th type, where  $n$  is the number of atom types, and  $\sum N_j = N$  is the total number of carbon atoms in the cage. The distribution of the atoms over atom types depends on both the topologies and geometries of the fullerene molecules that allow reflecting their symmetries [16]. The information entropy of the molecule ( $h$ ) equals the sum of the logarithms associated with each atom type [16,44]:

$$h = - \sum_{j=1}^n \frac{N_j}{\sum_{j=1}^n N_j} \log_2 \frac{N_j}{\sum_{j=1}^n N_j} \quad (2)$$

Herein, we use two as the base of the logarithms, which is conventional [7] and allows for expressing all information entropy values in bits. Single atoms have zero information entropy according to Equation (2) ( $n = 1$  and  $N_j = 1$ ).

Following Ugi and Gillespi [52], the chemical reaction is considered the 'isomerization' of one molecular ensemble (ME) to another. Hence, the change in information entropy upon the chemical process equals the difference between the  $h_{ME}$  values of two ensembles, products and reactants [14,44,53]:

$$\Delta h_R = h_{ME}^{prod} - h_{ME}^{react} \quad (3)$$

The information entropy of each ME is calculated as:

$$h_{ME} = H_{\Omega} + \sum_{i=1}^m \omega_i h_i \quad (4)$$

where  $\omega_i$  is the fraction of the  $i$ -th molecule in ME:

$$\omega_i = \frac{N_i}{\sum_{i=1}^m N_i} \quad (5)$$

and  $H_{\Omega}$  is the cooperative entropy:

$$H_{\Omega} = - \sum_{i=1}^m \omega_i \log_2 \omega_i \quad (6)$$

The  $H_{\Omega}$  is an emergent parameter that arises due to the mixing of molecules when they form the ensemble. It is independent from the molecular structure of the ME members

( $h_i$ ) and is defined only by their sizes ( $\omega_i$ ).  $H_\Omega = 0$  in the case of monomolecular ME (when  $\omega = 1$ ).

A combination of Equations (3) and (6) provides the following expression for information entropy changes in a chemical process:

$$\Delta h_R = H_{redistr} + H_{reorg} \quad (7)$$

where the first term is the redistribution information entropy, reflecting the difference in the size of the molecules in MEs of products and reactants:

$$H_{redistr} = H_\Omega^{prod} - H_\Omega^{react} \quad (8)$$

The second term, called reorganization information entropy, depends on both  $h_i$  and  $\omega_i$ , i.e., on structure and size, respectively:

$$H_{reorg} = \sum_i^{prod} \omega_i h_i - \sum_j^{react} \omega_j h_j \quad (9)$$

The last term can be further divided over two contributions:

$$H_{reorg}^{str} = \sum_i^{prod} h_i - \sum_j^{react} h_j \quad (10)$$

$$H_{reorg}^{str+size} = \sum_j^{react} (1 - \omega_j) h_j - \sum_i^{prod} (1 - \omega_i) h_i \quad (11)$$

Using this formalism, we can separately assess the changes in information entropy that correspond to molecular size and/or molecular structure. In Equations (7)–(11), the upper indices ‘*str*’ and ‘*size*’ indicate the references to molecular structure and size, respectively. Redistribution entropy  $H_{redistr}$  (Equation (8)) depends only on the size of the reaction participants. The explanatory remarks to this approach can be found in our key work [44] (the corresponding chemical and mathematical justifications are presented in earlier works [14,53]).

In brief, we list the information entropies used in the work and their designations. The  $h$  and  $h_{ME}$  values characterize the complexity of the molecules and molecular ensembles, respectively. The  $h_{ME}$  value contains cooperative entropy  $H_\Omega$  as a part. This is an emerging parameter that reflects the effect of uniting molecules in the ensemble. The information entropies with delta signs on designated with capital letters correspond to chemical processes ( $\Delta h_R$  and its components  $H_{redistr}$  and  $H_{reorg}$ ).

### 3.2. Structures of (Endo)Fullerenes for Analysis and Symmetry Determination

As mentioned in Section 2.1, the molecular graphs are necessary to obtain the information entropies of the fullerene molecules. To define the symmetries of the (endo)fullerenes, we used our previous works on (endo)fullerenes, whereby their structures were obtained with reliable density functional theory methods [16,17,38,39]. The symmetry point groups of chemical objects in this and our previous studies were determined in program Chemcraft [54].

## 4. Results

In this work, we consider three main cases of the process presented with Equation (1). The cases differ in what happens with the symmetry of the original (empty) fullerene cage (Figure 1). It can be served, increased or decreased depending on the chemical features of the interacting guest atom  $X$  and fullerene host  $C_N$ . Herein, the topology of the

fullerene cage does not change after filling. Additionally, we focus below on the analytical expressions for  $\Delta h_R$  and its components by providing numerical results.

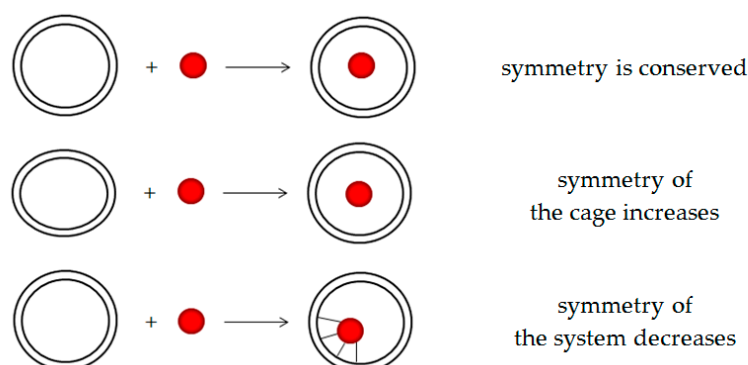


**Figure 1.** Three cases of the endofullerene formation (Equation (1)) depending on the relations between the symmetries of empty and filled fullerene cages.

#### 4.1. Introducing X into the Fullerene Cage: Common Analytical Expressions

Before starting a study, we briefly demonstrate the calculations of the information entropies of fullerene molecules using  $C_{60}$  ( $I_h$ ) and  $C_{70}$  ( $D_{5h}$ ) as examples (Figure 2). Their partitions are  $1 \times 60$  and  $3 \times 60 + 2 \times 20$ , respectively. The substitution of the populations of atom types to Equation (2) leads to the  $h$  values for these fullerenes, equal to 0 and 2.236 bits.

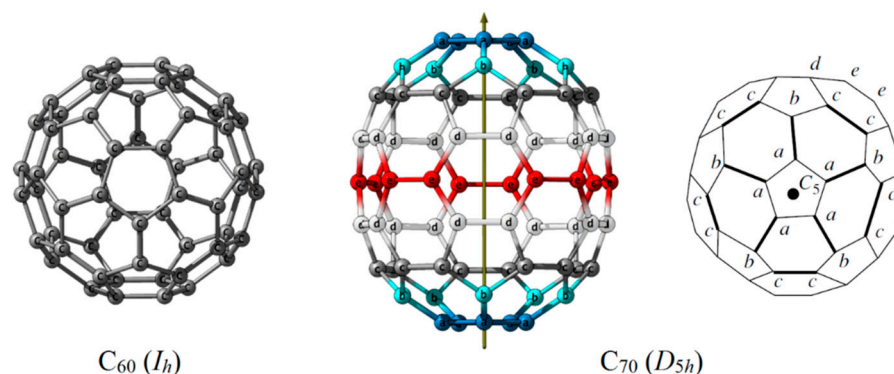


**Figure 2.** The partitions of the molecules of the two most abundant fullerenes over atom types. The  $C_{60}$  ( $I_h$ ) fullerene's atoms are shown in one color, as all of them belong to one atom type (**left**). In the case of  $C_{70}$  ( $D_{5h}$ ), atoms of different atom types are shown in different colors and designated with Latin letters (**center**). The attributions of  $C_{70}$ 's atoms are shown in a structural formula that corresponds to the top view on the molecule in the direction of its  $C_5$  symmetry axis (**right**).

In the case of introducing X into the  $C_N$  cage, we have the following input data for simplifying characteristic Equations (7)–(11): (a) the information entropy of the atom equals zero,  $h_X = 0$ ; and (b) the cooperative entropy of the molecular ensemble of the products is zero because the single product is formed under reaction (1),  $H_{\Omega}^{prod} = 0$ . The symmetry of the cage does not change (Figure 3) because atom X takes the position in the mass center of the cage, which coincides with the intersection of symmetry elements, if any.

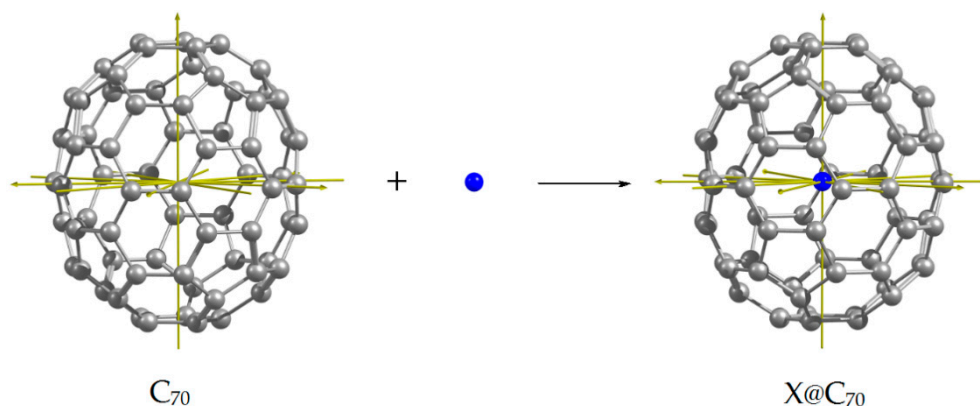


**Figure 3.** Formation of endohedral complexes of  $C_{70}$  ( $D_{5h}$ ) with conserving symmetry. The symmetry axes are shown as yellow arrows.

Considering the above, we obtain:

$$H_{redistr} = \frac{N}{N+1} \log_2 N - \log_2(N+1) \quad (12)$$

$$H_{reorg} = h_{X@C_N} - \frac{N}{N+1} h_{C_N} \quad (13)$$

$$H_{reorg}^{str+size} = \frac{1}{N+1} h_{C_N} \quad (14)$$

$$H_{reorg}^{str} = h_{X@C_N} - h_{C_N} \quad (15)$$

If the symmetry does not change, the partitions over atom types for  $X@C_N$  can be simply represented as  $1 \times 1 + \{\text{partition of } C_N\}$ . This allows rewriting Equation (13) as:

$$H_{reorg} = \log_2(N+1) - \frac{N}{N+1} \log_2 N \quad (16)$$

Thus,  $H_{reorg} = -H_{redistr}$  and  $\Delta h_R = 0$  (according to Equation (7)).

We present the work on the approach on endofullerenes in Table 1. Note that  $H_{redistr}$  depends only on the size of the filled fullerene, so this value is insensible towards the structural differences in the cases below. As the symmetry does not change upon the encapsulation, we may compare the structural effects of trapped atom  $X$  for different fullerenes. From the chemical point of view, as the fullerene cage becomes larger, the impact of trapped atom  $X$  on the system becomes smaller. In terms of information entropy, it means that  $H_{reorg}$  decreases with increasing  $N$ , which is observed in the calculated values (Table 1).

#### 4.2. Introducing $X$ into a Zero- $h$ Fullerene Cage While Serving Initial Symmetry

Fullerene  $C_{60}$  ( $I_h$ ) is the most prominent fullerene among other member of the fullerene family. It is the only fullerene molecule having zero information entropy calculated via Equation (2) due to the equivalence of all atoms [16]. Therefore, the case of  $h_{C_N} = 0$  deserves separate attention. The  $C_{60}$  cage is very stable, and, if there are no special interactions between the introduced guest atom  $X$  and the cage (e.g., charge transfer), the guest atom holds the position in the mass centrum of the cage. The cage is negligibly extended and serves its initial icosahedral symmetry. The mentioned situation is typical for the formation of noble gas endofullerenes [35–37,39].

**Table 1.** Information entropy indices of filling typical fullerenes (Equation (1)) with conserved symmetry (herein, all values are in bits).

Fullerene $C_N$ (Partition) <sup>a</sup>	$h_{C_N}$	$h_{X@C_N}$	$H_{reorg}^{str}$	$H_{reorg}^{str+size}$	$H_{reorg}$	$H_{redistr}$	$\Delta h_R$
$C_{20} (C_i)$ <sup>b</sup> (10 × 2)	3.3219	3.4399	0.1180	0.1582	0.2762	−0.2762	0
$C_{36-15} (D_{6h})$ (3 × 12)	1.5850	1.7214	0.1364	0.0428	0.1793	−0.1793	0
$C_{50-271} (D_{5h})$ (3 × 10 + 1 × 20)	1.9219	2.0235	0.1015	0.0377	0.1392	−0.1392	0
$C_{70-1} (D_{5h})$ (2 × 20 + 3 × 10)	2.2359	2.3112	0.0753	0.0315	0.1068	−0.1068	0
$C_{84-20} (T_d)$ (1 × 12 + 3 × 24)	1.9502	2.0195	0.0693	0.0229	0.0923	−0.0923	0
$C_{84-24} (D_{6h})$ (3 × 12 + 2 × 24)	2.2359	2.3019	0.0660	0.0263	0.0923	−0.0923	0

<sup>a</sup> The designations of the fullerene isomers are according to Atlas [45]. <sup>b</sup> The case of filling  $C_{20} (C_i)$  with enhancing symmetry is described in Section 4.4.

All carbon atoms in  $X@C_{60} (I_h)$  remain equivalent, and its partition is  $1 \times 1 + 1 \times 60$ , or  $1 \times 1 + 1 \times N$  in the general case for similar  $X@C_N$ . For the information entropy of  $X@C_N$ , we can write:

$$h_{X@C_N} = \log_2(N+1) - \frac{N}{N+1} \log_2 N \quad (17)$$

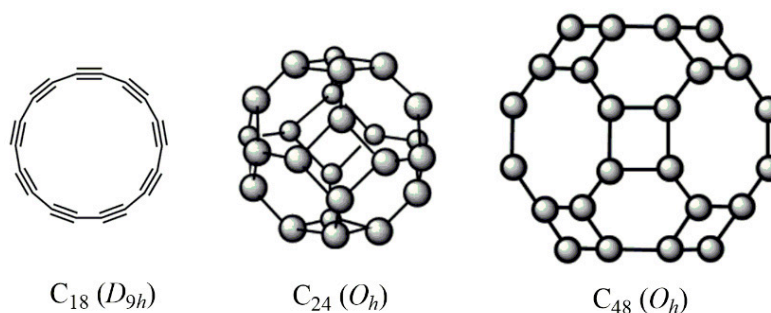
and it is obvious that  $h_{X@C_N} = -H_{redistr}$ , cf.: Equation (12). We obtain the same equations for  $H_{redistr}$  and  $H_{reorg}$  as in the case above; therefore,  $\Delta h_R = 0$ . However, the components of  $H_{reorg}$  differ:

$$H_{reorg}^{str} = \log_2(N+1) - \frac{N}{N+1} \log_2 N \quad (18)$$

$$H_{reorg}^{str+size} = 0, \quad (19)$$

i.e., there are no structural changes simultaneously depending on the molecular size and molecular structure.

In addition to zero- $h$  fullerene  $C_{60}$ , we consider other carbon molecules having  $h = 0$ , which can form complexes in a similar way (with placing guest atom in the central position). These are the hypothetical fullerene-like molecules  $C_{24} (O_h)$  and  $C_{48} (O_h)$ , containing polygons untypical for fullerenes (tetra- and octagons) [47,55], and synthesized cyclo [18] carbon  $C_{18}$  has a  $D_{9h}$  symmetry [56] (Figure 4). The numerical results obtained for  $C_{60} (I_h)$  and these structures are shown in Table 2.

**Figure 4.** Carbon structures having all atoms equivalent and, hence, zero information entropy: synthesized cyclo[18]carbon  $C_{18} (D_{9h})$  and hypothetical fullerene-like cages  $C_{24} (O_h)$  and  $C_{48} (O_h)$ .

**Table 2.** Information entropy indices of zero- $h$  carbon species forming complexes with X with conserved symmetry.

Carbon Molecule	$h_{C_N}$	$h_{X@C_N}$	$H_{reorg}^{str}$	$H_{reorg}^{str+size}$	$H_{reorg}$	$H_{redistr}$	$\Delta h_R$
Fullerene C <sub>60</sub> ( $I_h$ )	0	0.1207	0.1207	0	0.1207	−0.1207	0
Fulleroid C <sub>24</sub> ( $O_h$ )	0	0.2423	0.2423	0	0.2423	−0.2423	0
Fulleroid C <sub>48</sub> ( $O_h$ )	0	0.1437	0.1437	0	0.1437	−0.1437	0
Cyclocarbon C <sub>18</sub> ( $D_{9h}$ )	0	0.2975	0.2975	0	0.2975	−0.2975	0

#### 4.3. Introducing X into Maximum- $h$ Fullerene Cage

Symmetric fullerenes are the main products of arc-discharge fullerene synthesis [57]. Moreover, there are examples of fullerenes with no symmetry, whose molecules are attributed to the  $C_1$  symmetry point group (e.g., see [58–61]). Additionally, the majority of the hypothetical fullerene structures belong to this type [16,45]. For these fullerenes, information entropy achieves its maximal value for a given  $N$  (which corresponds to the partition of the molecule  $N \times 1$ ) [16]:

$$h_{C_N (C_1)} = \log_2 N \quad (20)$$

The application of Equation (20) to expressions (7)–(11) after some simplifications affords the same equations for  $H_{redistr}$  and  $H_{reorg}$ , as in the two cases above, and, consequently,  $\Delta h_R = 0$ . The components of  $H_{reorg}$  are the following:

$$H_{reorg}^{str} = \log_2(N + 1) - \log_2 N \quad (21)$$

$$H_{reorg}^{str+size} = \frac{1}{N + 1} \log_2 N \quad (22)$$

As can be seen, they differ from the case of the zero- $h$  fullerene, as the reorganization entropy is divided over two contributions ( $H_{reorg}^{str+size} = 0$  in the case of  $h_{C_N} = 0$ ). As for the comparison with the case of Section 3.1, here,  $H_{reorg}^{str+size}$  achieves its maximal value due to condition (20). Some typical numerical examples of this case are collected in Table 3.

**Table 3.** Information entropy indices of maximum- $h$  fullerenes filled with X (systems with  $C_1$  symmetry).

Fullerene C <sub>N</sub>	$h_{C_N}$	$h_{X@C_N}$	$H_{reorg}^{str}$	$H_{reorg}^{str+size}$	$H_{reorg}$	$H_{redistr}$	$\Delta h_R$
C <sub>60</sub>	5.9069	5.9307	0.0239	0.0968	0.1207	−0.1207	0
C <sub>70</sub>	6.1293	6.1497	0.0205	0.0863	0.1068	−0.1068	0
C <sub>80</sub>	6.3219	6.3399	0.0179	0.0780	0.0960	−0.0960	0
C <sub>90</sub>	6.4919	6.5078	0.0159	0.0713	0.0873	−0.0873	0

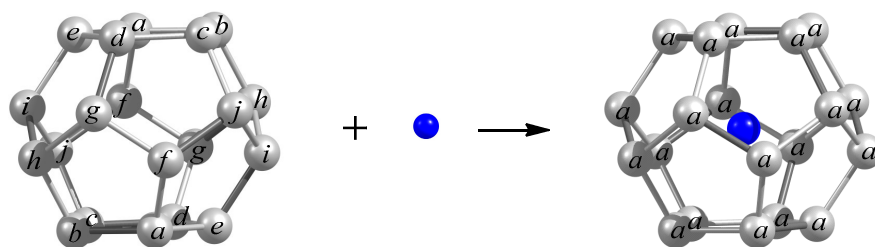
#### 4.4. Introducing X into the Fullerene Cage with Initially Reduced Symmetry

Some of the fullerenes, especially nonconventional structures, reveal Jahn–Teller symmetry reduction [47]. We do not discuss here its molecular–orbital reasons, and we instead focus on the consequences that are important for the present study. The topology of the fullerene cage undergoing the effect remains the same, but spatially, the structure is distorted; therefore, the actual symmetry becomes lower compared to the ideal symmetry deduced from the topology [16,47]. The C<sub>20</sub> fullerene is a typical example of such a fullerene. Its ideal symmetry is  $I_h$ , but it is reduced to the Jahn–Teller effect to  $C_i$  [62]. (Note that the actual symmetry of C<sub>20</sub> is questionable because different quantum–chemical approximations predict different symmetries,  $C_2$ ,  $C_{2h}$ ,  $C_i$ ,  $D_{3d}$  and  $D_{2h}$  [47]. All of them are lower than  $I_h$ . We use the  $C_i$  symmetry structure as obtained in our previous work [62].) Other representatives of fullerenes of this type are listed in Table 4.

**Table 4.** Information entropy of fullerene structures with Jahn–Teller symmetry reduction and their endohedral complexes, in which the effect vanishes.

Fullerene $C_N$	Idealized Symmetry	Actual Symmetry	$h_{C_N}^{ideal}$	$h_{X@C_N}^{ideal}$	$h_{C_N}$
$C_{20-1}$	$I_h (1 \times 20)$	$C_i (10 \times 2)$	0.0000	0.2762	3.3219
$C_{24-1}$	$D_{6d} (2 \times 12)$	$C_2 (12 \times 2)$	1.0000	1.2023	3.5850
$C_{26-1}$	$D_{3h} (1 \times 2 + 2 \times 6 + 1 \times 12)$	$C_1 (26 \times 1)$	1.7759	1.9386	4.7004
$C_{40-1}$	$D_{5d} (4 \times 10)$	$C_i (20 \times 2)$	2.0000	2.1166	4.3219
$C_{76-2}$	$T_d (1 \times 4 + 2 \times 12 + 2 \times 24)$	$S_4 (3 \times 4 + 4 \times 8 + 2 \times 16)$	2.1148	2.1873	2.9848
$C_{80-7}$	$I_h (1 \times 20 + 1 \times 60)$	$C_{3v} (1 \times 2 + 1 \times 6 + 6 \times 12)$	0.8113	0.8972	2.8766

Filling the  $C_{20}$  ( $C_i$ ) cage with noble gas atoms (He or Ne) leads to expanding the cage but does not change its symmetry, i.e., He@ $C_{20}$  and Ne@ $C_{20}$  are also  $C_i$  symmetry structures [35–39]. However, if metal species such as Nd, U, Pm<sup>+</sup>, Np<sup>+</sup>, Sm<sup>2+</sup>, Pu<sup>2+</sup>, Eu<sup>3+</sup>, Am<sup>3+</sup>, Gd<sup>4+</sup> or Cm<sup>4+</sup> play the role of guest atoms, the  $C_{20}$  cages obtain icosahedral symmetry. A metal guest takes the place at the center of the cage, so the formed X@ $C_{20}$  structures are  $I_h$ -symmetric [63]. This is reflected in Figure 5.

**Figure 5.** Formation of X@ $C_{20}$  ( $I_h$ ) from  $C_{20}$  ( $C_i$ ) and X. The attributions of carbon atoms in the fullerene cages are shown with Latin letters.

A similar ideal symmetry restoration within the endohedral complexes may be typical for other fullerenes, which demonstrate the Jahn–Teller symmetry reduction in the empty state (e.g.,  $C_{24-1}$ ,  $C_{26-1}$ ,  $C_{40-1}$ ,  $C_{76-2}$  and  $C_{80-7}$  [16], the designation after the hyphen is the number of the isomer according to Atlas [45]). The corresponding information entropy changes, and their contributions are described with Equations (12)–(16) (Table 5). Herein, the relation is typical for this type of formed endofullerene (Table 4):

$$h_{C_N} > h_{X@C_N}^{ideal} \equiv h_{X@C_N} > h_{C_N}^{ideal} \quad (23)$$

where the upper index ‘ideal’ indicates that the fullerene cage is in the highest symmetry state possible for the given topology. Due to the above inequality,  $H_{redistr} \neq H_{reorg}$ ; therefore, the resulting  $\Delta h_R$  values are negative in contrast to the cases considered above with unchanged symmetry. The information entropy changes in such processes are calculated as:

$$\Delta h_R = h_{X@C_N} - \frac{N}{N+1} (h_{C_N} - \log_2 N) - \log_2(N+1) < 0 \quad (24)$$

**Table 5.** Information entropy indices of filling fullerenes accompanied with increasing symmetry of the fullerene cage.

Fullerene $C_N$	$H_{reorg}^{str}$	$H_{reorg}^{str+size}$	$H_{reorg}$	$H_{redistr}$	$\Delta h_R$
$C_{20-1}$ ( $C_i \rightarrow I_h$ )	−3.0457	0.1582	−2.8875	−0.2762	−3.1637
$C_{24-1}$ ( $C_2 \rightarrow D_{6d}$ )	−2.3827	0.1434	−2.2393	−0.2423	−2.4816
$C_{26-1}$ ( $C_1 \rightarrow D_{3h}$ )	−2.7618	0.1741	−2.5877	−0.2285	−2.8163
$C_{40-1}$ ( $C_i \rightarrow D_{5d}$ )	−2.2053	0.1054	−2.0999	−0.1654	−2.2653
$C_{76-2}$ ( $S_4 \rightarrow T_d$ )	−0.7974	0.0388	−0.7587	−0.1000	−0.8587
$C_{80-7}$ ( $C_{3v} \rightarrow I_h$ )	−1.9794	0.0355	−1.9438	−0.0960	−2.0398



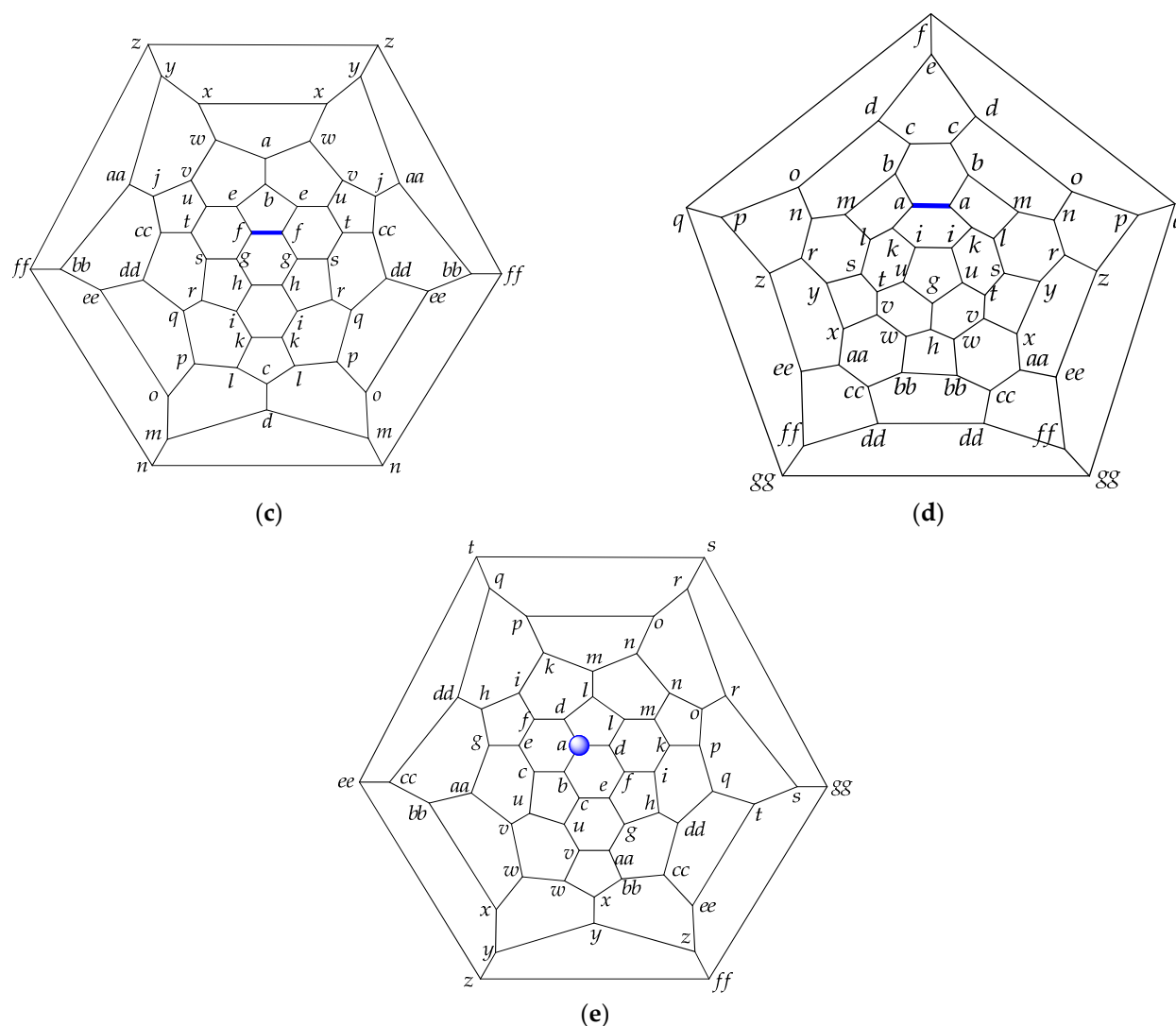


**Figure 7.** Schlegel diagrams of  $X@C_{60}$  with coordination  $X$  via (a) hexagon, (b) pentagon, (c) 5.6 bond, (d) 6.6 bond and (e) atom of the fullerene cage. These elements of the fullerene structure are shown in blue. The carbon atoms of different atom types are lettered.

**Table 6.** Information entropy indices of filling  $C_{60}$  ( $I_h$ ) with  $X$  coordination relative to the cage.

Coordination of X Atom inside $C_{60}$	Symmetry of $X@C_{60}$ and Partition	$H_{reorg}=H_{reorg}^{str}=h_{X@C_{60}}$	$H_{redistr}$	$\Delta I_R$
Pentagon	$C_{5v}$ ( $4 \times 5 + 4 \times 10 + 1 \times 1$ )	2.991	-0.1207	+2.870
Hexagon	$C_{3v}$ ( $8 \times 6 + 4 \times 3 + 1 \times 1$ )	3.585	-0.1207	+3.464
5.6-bond	$C_5$ ( $5 \times 1 + 28 \times 2$ )	5.013	-0.1207	+4.892
6.6-bond	$C_{2v}$ ( $5 \times 1 + 28 \times 2$ )	5.013	-0.1207	+4.892
Atom	$C_5$ ( $5 \times 1 + 28 \times 2$ )	5.013	-0.1207	+4.892

The above considerations are applicable to other fullerenes in the same way. Other fullerenes have lower symmetries; therefore, endo-atom  $X$  may be coordinated towards a larger number of the substructures of the fullerene cage (but their types are the same as in the described  $C_{60}$  case of pentagons, hexagons, atoms and 5.6- and 6.6-bonds). Note that our approach does not distinguish topological isomers  $X@C_N$  and  $X \dots C_N$ , i.e., the isomers differ in the  $X$  location, inside or outside the cage. Therefore, the obtained relations are also characteristic for exohedral fullerene complexes, another class of fullerene compounds [68].

#### 4.6. Information Entropy Indices of Processes $X + C_N \rightarrow X@C_N$ within Series of Isomeric Fullerenes

A number of isomeric fullerene structures may correspond to each molecular size ( $N$ ), and the task of comparing fullerene isomers often arises in fullerene science. Therefore, we explore this case for two fullerene series taken from our previous works [15,16]. The original symmetry of the fullerene cage is conserved under encapsulation. As follows from Section 4.1,  $\Delta h_R = 0$  and  $H_{reorg} = -H_{redistr} = f(N)$  are the same for the endofullerene formation within the isomeric series. Hence, we focus on the  $H_{reorg}^{str}$  values, which are distinctive for the isomers.

Before mathematical treatment, we consider some chemical aspects of process (1) regarding the behavior of information entropy. These processes share one common feature: the symmetry of the cage is the same in empty and encapsulated states. The difference between the processes in each isomeric series is due to the symmetry of certain fullerene molecules. At first glance, it seems that the  $H_{reorg}^{str}$  values (calculated via Equation (15)) should be the same for different fullerenes isomers. However, in fact, the  $H_{reorg}^{str}$  values for the selected  $C_{60}$  isomers differ (Table 7). Herein, as the symmetry of the fullerene isomer becomes higher,  $H_{reorg}^{str}$  becomes larger. Note that, as a preliminary example, to find a pattern, we use a series of only six isomers of  $C_{60}$  that have different symmetries (their total number equals 1812 [69]). As follows from Table 7, the rotational symmetry number is not the best mode to quantify the fullerene symmetry. Indeed,  $\sigma = 2$  for  $C_{60}$  ( $C_{2v}$ ) and  $C_{60}$  ( $C_2$ ), but these isomers differently crumble over atom types. For further work, we need to use some quantity that numerically catches the differences in the partitions of the fullerene isomers.

**Table 7.** Information entropy indices of filling  $C_{60}$  isomer with different symmetries.

Isomer	Partition	$\sigma$	$\chi$	$h_{C_N}$	$h_{X@C_N}$	$H_{reorg}^{str}$
$C_{60}$ ( $I_h$ )	$1 \times 60$	30	354.4	0.000	0.121	0.121
$C_{60}$ ( $D_{5d}$ )	$2 \times 20 + 2 \times 10$	10	239.3	1.918	2.008	0.089
$C_{60}$ ( $D_{2h}$ )	$3 \times 4 + 6 \times 8$	4	168	3.107	3.177	0.070
$C_{60}$ ( $C_{2v}$ )	$6 \times 2 + 12 \times 4$	2	108	4.107	4.160	0.053
$C_{60}$ ( $C_2$ )	$30 \times 2$	2	60	4.907	4.947	0.040
$C_{60}$ ( $C_1$ )	$60 \times 1$	1	0	5.907	5.931	0.024

By scrutinizing isomeric series with  $N = \text{const}$ , we introduce logarithmic partition number ( $\chi$ ) for convenience:

$$\chi = \sum_{j=1}^n N_j \log_2 N_j \quad (25)$$

It characterizes the partition and correlates with  $\sigma$  (Figure 8), and the information entropies of (endo)fullerenes are expressed with  $\chi$  (combining Equations (2) and (25)):

$$h_{C_N} = \log_2 N - \frac{\chi}{N} \quad (26)$$

$$h_{X@C_N} = \log_2(N + 1) - \frac{\chi}{N + 1} \quad (27)$$

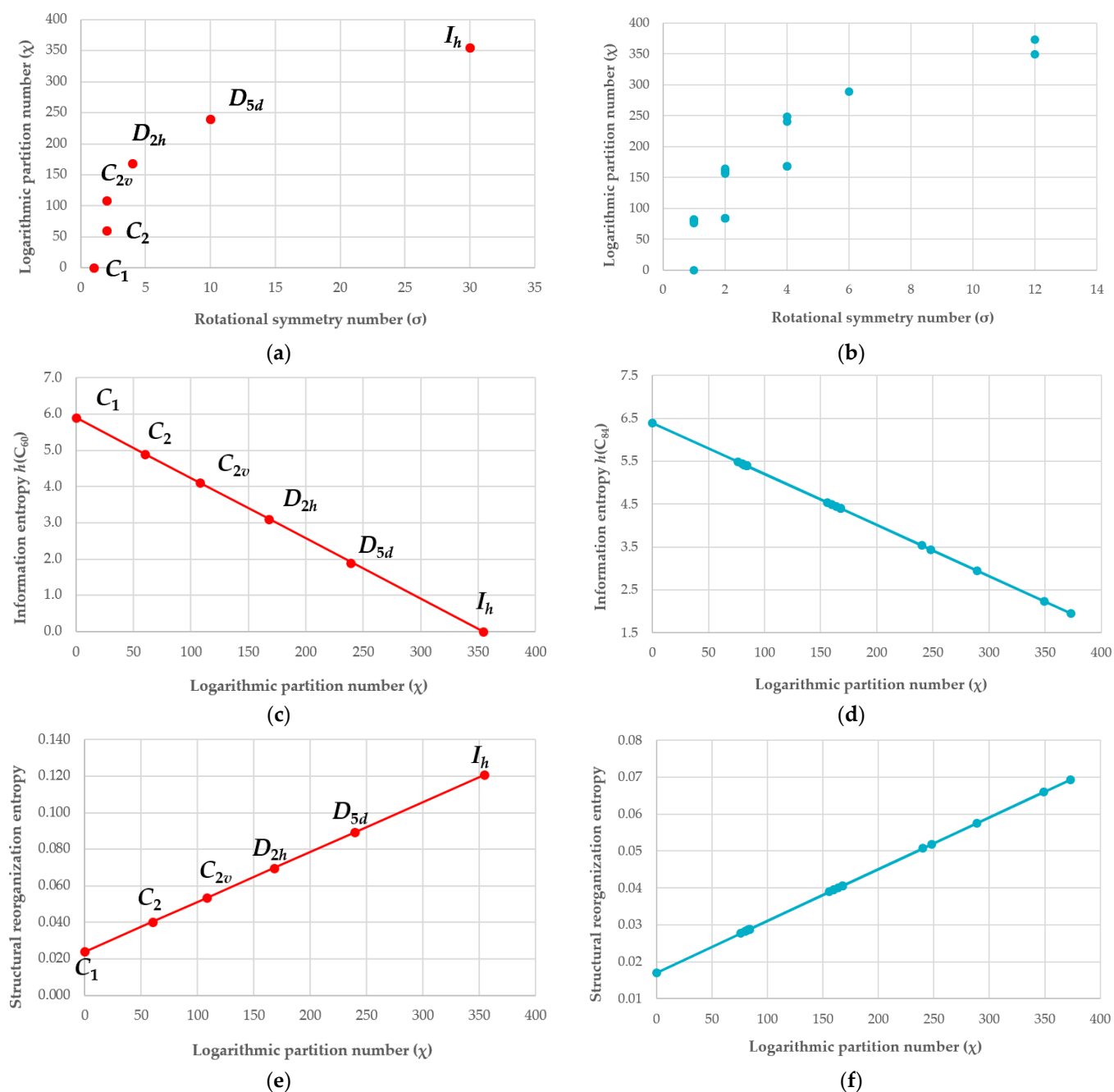


**Figure 8.** Information entropy and symmetry indices of processes  $X + C_N \rightarrow X@C_N$  within series of isomeric fullerenes C<sub>60</sub> (a,c,e) and C<sub>84</sub> (b,d,f). Numerical data associated with the plot can be found in Table 7 and Supplementary Materials.

Importantly, minimal  $\chi$  equals zero and corresponds to the lowest symmetry (C<sub>1</sub>), whereas  $\chi_{\max} = N \log_2 N$  corresponds to a high symmetry (I<sub>h</sub> in the C<sub>60</sub> series). In general,  $\chi \rightarrow 0$  if the partition of the molecule includes singly populated atom types, i.e., when  $n \rightarrow N$  and  $N_j \rightarrow 1$ . In the opposite case, when the atom types are highly populated, we have  $n \rightarrow 1$ ,  $N_j \rightarrow N$  and  $\chi \rightarrow \chi_{\max}$ .

Substituting expressions (26) and (27) into Equation (15) provides linear dependence for structural reorganization entropy on the logarithmic partition number:

$$H_{reorg}^{str} = \log_2 \frac{N+1}{N} + \frac{\chi}{N(N+1)} \quad (28)$$

According to the last expression,  $H_{reorg}^{str}$  increases with  $\chi$  (Figure 8). As  $\chi$  is connected with a linear equation and with the information entropy of fullerenes and correlates with their symmetries, we can interpret Equation (28) in terms of both symmetry and information entropy. As the information entropy of the fullerene become smaller, its symmetry becomes higher, and the structural changes expressed with  $H_{reorg}^{str}$  become larger. In other words, the information entropy associated with structural changes at the endofullerene formation depends on the symmetry of the original structure.

To demonstrate that the discussed statements are valid in other cases, we have also applied them to the series of isolated pentagon isomers of  $C_{84}$ . As seen in Figure 8, the correlations between  $\chi$  and  $\sigma$  becomes worse in this wider series, but these values remain symbatic. In general,  $\chi$  provides more diversified numerical assessing chemical structures as compared with  $\sigma$ . The use of the logarithmic partition number allows for generalizing the above cases (substituting  $\chi_{max}$  and  $\chi_{min}$  in Equation (28) leads to Equations (18) and (21) for zero- $h$  and maximum- $h$  fullerenes, respectively).

## 5. Discussion

### 5.1. General Remarks

We have applied our original information entropy approach to describe the relations between chemical structure and symmetry upon filling fullerene cages with guest atom  $X$ . The obtained numerical data are well interpretable in terms of general chemical notions. Herein, we have operated this total information entropy change both in the process and its components.

The total change  $\Delta h_R$  allows for discriminating the cases when symmetry is changed upon the title process;  $\Delta h_R$  is negative, positive or zero if symmetry is increased, reduced or does not change, respectively. Furthermore, the components of  $\Delta h_R$  correspond to the types of empty fullerenes and formed endofullerenes, and this correspondence is unambiguous. Thus, we state here that the type of the (endo)fullerene structure can be deduced from the information entropy estimates of process (1). It can be performed digitally using the algorithm based on comparing  $\Delta h_R$  and  $H_{reorg}^{str+size}$  values (Figure 9). Information-entropy-based classifications have been elaborated to sort natural compounds [25] and interstellar [13] and isentropic molecules [70], and they have operated with numerical estimates of chemical structures. We propose a scheme (Figure 9) utilizing indices relating to the process, which involves chemical structures. Such tasks are currently not widespread in mathematical chemistry. Deciphering the chemical structure based on the information about its chemical processes is standard for classical (experimental) chemistry. Therefore, we can assume that the digital task, similar to that one, will arise in chemical sciences in the nearest future.

### 5.2. Dependence of the Structural Reorganization Entropy of Encapsulation on the Symmetry and Size of Fullerenes

The main aim of this proposed concept is developing an information entropy approach applicable to all molecular compounds. We focus on fullerenes because they are rigid and symmetric molecules that are very convenient for testing structural descriptors and linking numerical estimates with chemical notions. Information entropy and symmetry are concepts closely relating to molecular complexity. High information entropy corresponds to low symmetry and high complexity of the molecules [2,16].

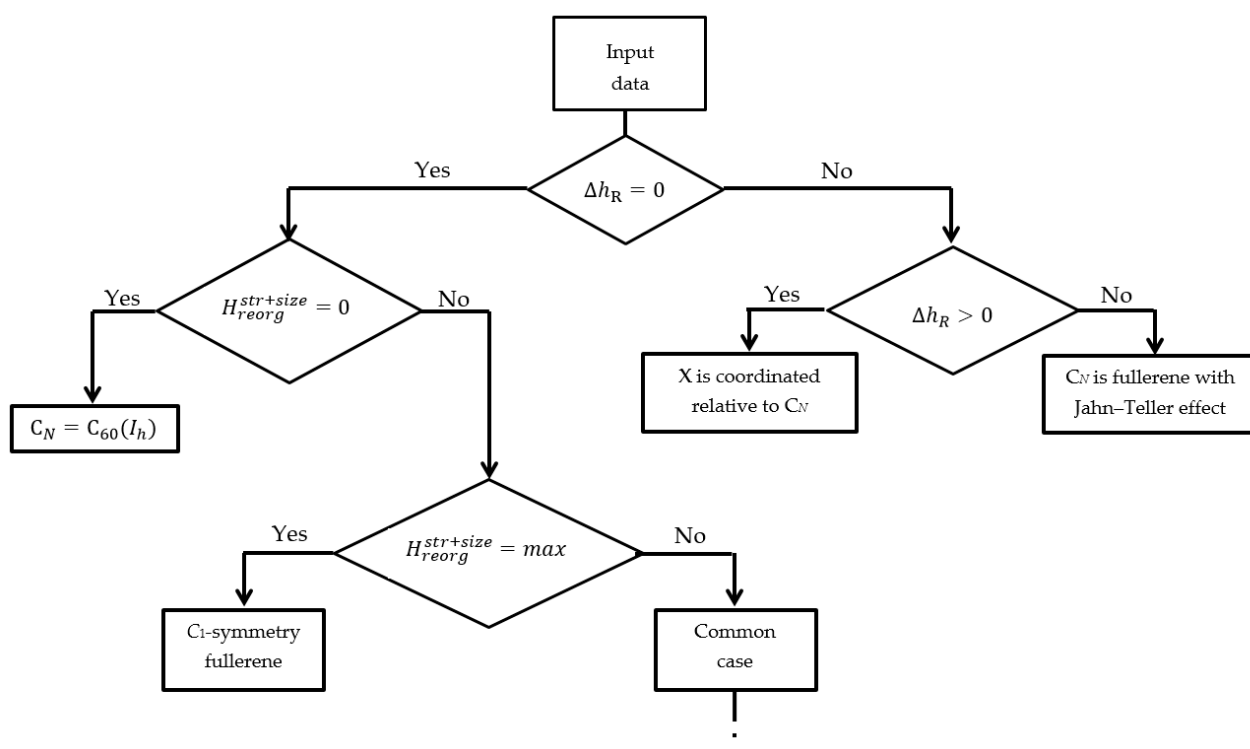


**Figure 9.** Algorithm for deducing the type of (endo)fullerene from the numerical information entropy estimates of process  $X + C_N \rightarrow X@C_N$ , in which it is involved. The input data contain  $\Delta h_R$  and its components.

The most interesting thing we have found in this work is that the information entropy of the intact fullerene  $h_{C_N}$  influences the structural reorganization entropy  $H_{reorg}^{str+size}$  of its filling. This finding is not obvious in the context of chemical intuition, and, therefore, we discuss it below.

If the symmetry remains unchanged, we have similar substrates involved in the identical processes, resulting in similar products (Equation (1)). The similarity of the processes is reflected by the equality of their  $\Delta h_R$  values ( $\Delta h_R = 0$ ), and this is well understandable. At first glance, numerical estimates associated with structural changes ( $H_{reorg}^{str+size}$ ) for these processes should also be equal, but, in fact, they are not the same. We rationalize this inequality using the logarithmic partition number  $\chi$  as an auxiliary parameter. The  $\chi$  number linearly linked with the information entropy correlates with the symmetry of the fullerene. As  $\chi$  becomes larger, the number of equivalent atoms in the molecule becomes larger, and as the  $h$  value becomes lower, its symmetry and the  $H_{reorg}^{str+size}$  of the encapsulation become higher. The latter means that, if the symmetry of the fullerene is high, the guest atom introduces more structural changes when encapsulated and vice versa. In symmetrical fullerene structures, the number of atom types is low, and they are highly populated. Filling them with  $X$  crashes this uniformity. In contrast, there are many sparsely populated atom types in low-symmetry structures, i.e., they have some degree of disorder before encapsulation, and the next additional atom in the system makes a small contribution to the structural complexity increase.

Thus, the information entropy of the empty fullerene defines the structural reorganization entropy of the encapsulation process. Taking into account the fact that information entropy reflects the complexity of the molecular system, we can propose a stronger version of this statement: the complexity of the initial structure defines the complexity change during the chemical reaction. The last sentence should be accepted as the assumption that requires further justification with other chemical compounds, chemical reactions and complexity measures.

Structural reorganization entropy  $H_{reorg}^{str+size}$  also depends on the size of the fullerene cage expressed with  $N$ . By analyzing fullerenes with different  $N$  (Tables 1–3 and 5), one can find that the  $H_{reorg}^{str+size}$  decreases  $N$ . This means that the structural changes relating to introducing the endo-atom to the molecular system becomes smaller in the background of the whole. This fits into the previously found regularities for chemical reactions in homological series of hydrocarbons and their derivatives [14,44].

### 5.3. Perspectives

The approach used in the present work is quite new, and we are going to extrapolate it to other chemical systems and processes involving fullerenes, including chemical processes, e.g., filling fullerenes with two or more atoms, multi-atomic clusters or small molecules. Such endofullerenes are currently being synthesized (e.g.,  $H_2O@C_{60/70}$ ,  $He_2@C_{60/70}$ ,  $HeN@C_{60/70}$ ,  $Sc_3N@C_N$ ,  $M_2C_2@C_N$ ) (see works [71–73] and the references therein). We also think that the approach could be useful for the analysis of exohedral additions to fullerenes [68,74,75], where information entropy is expected to catch both the complexity of the addition pattern [74] and the symmetry of functional groups attached to the fullerene cage [75].

In a recent review, we point out that the information entropy concept is a good value for interdisciplinary studies, as it has applications in various fields [7]. In the present work, we have used it only as a structural descriptor, which could be further incorporated into the studies on planning syntheses [76], self-assembly processes [21–24] and informational [77–79] and geometrical [80] thermodynamics. This may be insightful for the interface between structural chemistry, physics and information sciences.

## 6. Conclusions

We have studied all cases of introducing one guest atom into the fullerene cage, forming endofullerenes in terms of original information entropy formalism. As has been found, the calculated total information entropy change reflects the structure and symmetry changes of the process, whereas its components can be used for the digital identification of key structural features of fullerenes participating in the process of filling.

We point out the importance of structural reorganization entropy (a part of the total information entropy change), and it depends on the structure and size of fullerenes. As the information entropy of an empty fullerene becomes lower, the  $H_{reorg}^{str+size}$  value becomes larger. The latter means that, in terms of symmetry, as the symmetry of the fullerene cage becomes higher, the structural changes due to filling it with a guest atom become larger.

In the future, we plan to apply the developed formalism to various reactions of organic compounds (including organic derivatives of fullerenes). The processes studied in the present work are simple in the following sense: only one atom is specifically introduced to a chemical system, with minimal symmetry changes and unchanged topology of the cage. This allows for rationalizing the structural meaning of the contributions to the information entropy change, which is important for more complex cases.

**Supplementary Materials:** The following supporting information can be downloaded at: <https://www.mdpi.com/article/10.3390/sym14091800/s1>, Table S1: Numerical data on the formation of endofullerenes  $X@C_{84}$  associated with Figure 8.

**Author Contributions:** Conceptualization, D.S.S.; methodology, D.S.S.; validation, A.A.T. and I.S.S.; formal analysis, D.S.S.; investigation, A.A.T.; writing—original draft preparation, D.S.S.; writing—review and editing, I.S.S.; visualization, A.A.T.; project administration, D.S.S.; funding acquisition, D.S.S. All authors have read and agreed to the published version of the manuscript.

**Funding:** This research was funded by the Russian Science Foundation, project “Information entropy of chemical reactions: A novel methodology for digital organic chemistry”, grant number 22-13-20095.

**Institutional Review Board Statement:** Not applicable.

**Informed Consent Statement:** Not applicable.

**Data Availability Statement:** Not applicable.

**Conflicts of Interest:** The authors declare no conflict of interest.

## References

1. Stankevich, M.I.; Stankevich, I.V.; Zefirov, N.S. Topological indices in organic chemistry. *Russ. Chem. Rev.* **1988**, *57*, 191–208. [[CrossRef](#)]
2. Bonchev, D. Kolmogorov's information, Shannon's entropy, and topological complexity of molecules. *Bulg. Chem. Commun.* **1995**, *28*, 567–582.
3. Barigye, S.J.; Marrero-Ponce, Y.; Pérez-Giménez, F.; Bonchev, D. Trends in information theory-based chemical structure codification. *Mol. Divers.* **2014**, *18*, 673–686. [[CrossRef](#)] [[PubMed](#)]
4. Basak, S.C.; Harriss, D.K.; Magnuson, V.R. Comparative study of lipophilicity versus topological molecular descriptors in biological correlations. *J. Pharm. Sci.* **1984**, *73*, 429–437. [[CrossRef](#)]
5. Basak, S.C.; Gute, B.D.; Grunwald, G.D. Use of topostructural, topochemical, and geometric parameters in the prediction of vapor pressure: A Hierarchical QSAR approach. *J. Chem. Inf. Comput. Sci.* **1997**, *37*, 651–655. [[CrossRef](#)]
6. Böttcher, T. An additive definition of molecular complexity. *J. Chem. Inf. Model.* **2016**, *56*, 462–470. [[CrossRef](#)]
7. Sabirov, D.S.; Shepelevich, I.S. Information entropy in chemistry: An overview. *Entropy* **2021**, *23*, 1240. [[CrossRef](#)]
8. Nagaraj, N.; Balasubramanian, K. Three perspectives on complexity: Entropy, compression, subsymmetry. *Eur. Phys. J. Spec. Top.* **2017**, *226*, 3251–3272. [[CrossRef](#)]
9. Krivovichev, S.V. Structural complexity of minerals: Information storage and processing in the mineral world. *Mineral. Mag.* **2013**, *77*, 275–326. [[CrossRef](#)]
10. Krivovichev, S.V. Structure description, interpretation and classification in mineralogical crystallography. *Crystallogr. Rev.* **2017**, *23*, 2–71. [[CrossRef](#)]
11. Krivovichev, S.V.; Krivovichev, V.; Hazen, R.M.; Aksenov, S.M.; Avdontceva, M.S.; Banaru, A.M.; Gorelova, L.A.; Ismagilova, R.M.; Korniyakov, I.V.; Kuporev, I.V.; et al. Structural and chemical complexity of minerals: An update. *Mineral. Mag.* **2022**, *86*, 183–204. [[CrossRef](#)]
12. Banaru, A.M.; Aksenov, S.M. Complexity of molecular nets: Topological approach and descriptive statistics. *Symmetry* **2022**, *14*, 220. [[CrossRef](#)]
13. Sabirov, D.S. Information entropy of interstellar and circumstellar carbon-containing molecules: Molecular size against structural complexity. *Comput. Theor. Chem.* **2016**, *1097*, 83–91. [[CrossRef](#)]
14. Sabirov, D.S. Information entropy changes in chemical reactions. *Comput. Theor. Chem.* **2018**, *1123*, 169–179. [[CrossRef](#)]
15. Sabirov, D.S.; Ori, O.; László, I. Isomers of the C<sub>84</sub> fullerene: A theoretical consideration within energetic, structural, and topological approaches. *Fuller. Nanotub. Carbon Nanostruct.* **2018**, *26*, 100–110. [[CrossRef](#)]
16. Sabirov, D.S.; Osawa, E. Information entropy of fullerenes. *J. Chem. Inf. Model.* **2015**, *55*, 1576–1584. [[CrossRef](#)]
17. Sabirov, D.S.; Terentyev, A.O.; Sokolov, V.I. Activation energies and information entropies of helium penetration through fullerene walls. Insights into the formation of endofullerenes nX@C<sub>60/70</sub> (n = 1 and 2) from the information entropy approach. *RSC Adv.* **2016**, *6*, 72230–72237. [[CrossRef](#)]
18. Sabirov, D.S.; Ori, O.; Tukhbatullina, A.A.; Shepelevich, I.S. Covalently bonded fullerene nano-aggregates (C<sub>60</sub>)<sub>n</sub>: Digitalizing their energy-topology-symmetry. *Symmetry* **2021**, *13*, 1899. [[CrossRef](#)]
19. Banaru, A.; Aksenov, S.; Krivovichev, S. Complexity parameters for molecular solids. *Symmetry* **2021**, *13*, 1399. [[CrossRef](#)]
20. Sabirov, D.S.; Ori, O.; Tukhbatullina, A.A.; Shepelevich, I.S. Structural descriptors of benzenoid hydrocarbons: A mismatch between the estimates and parity effects in helicenes. *C* **2022**, *8*, 42. [[CrossRef](#)]
21. Aleskovskii, V.B. *Chemical and Information Synthesis. The Beginnings of the Theory. Methods*; Publishing House of St. Petersburg University: St. Petersburg, Russia, 1997; 72p.
22. Talanov, V.M.; Ivanov, V.V. Structure as the source of information on the chemical organization of substance. *Russ. J. Gen. Chem.* **2013**, *83*, 2225–2236. [[CrossRef](#)]
23. Bal'makov, M.D. Information basis of nanochemistry. *Russ. J. Gen. Chem.* **2002**, *72*, 1023–1030. [[CrossRef](#)]
24. Kadomtsev, B.B. Dynamics and information. *Phys. Uspekhi* **1994**, *37*, 425–499. [[CrossRef](#)]
25. Castellano, G.; González-Santander, J.L.; Lara, A.; Torrens, F. Classification of flavonoid compounds by using entropy of information theory. *Phytochemistry* **2013**, *93*, 182–191. [[CrossRef](#)]
26. Feng, B.; Zhuang, X. Carbon-enriched meso-entropy materials: From theory to cases. *Acta Chim. Sin.* **2020**, *78*, 833–847. [[CrossRef](#)]
27. Krivovichev, S.V. Structural complexity and configurational entropy of crystals. *Acta Crystallogr. B Struct. Sci. Cryst. Eng. Mater.* **2016**, *72*, 274–276. [[CrossRef](#)]
28. Jiménez-Ángeles, F.; Odriozola, G.; Lozada-Cassou, M. Entropy effects in self-assembling mechanisms: Also a view from the information theory. *J. Mol. Liq.* **2011**, *164*, 87–100. [[CrossRef](#)]
29. Champion, Y.; Thurieau, N. The sample size effect in metallic glass deformation. *Sci. Rep.* **2020**, *10*, 10801. [[CrossRef](#)]
30. Popov, A.A.; Yang, S.; Dunsch, L. Endohedral fullerenes. *Chem. Rev.* **2013**, *113*, 5989–6113. [[CrossRef](#)]
31. Liu, S.; Sun, S. Recent progress in the studies of endohedral metallofullerenes. *J. Organomet. Chem.* **2000**, *599*, 74–86. [[CrossRef](#)]

32. Akhanova, N.Y.; Shchur, D.V.; Pomytkin, A.P.; Zolotareno, A.D.; Zolotareno, A.D.; Gavrylyuk, N.A.; Ualkhanova, M.; Bo, W.; Ang, D. Methods for the synthesis of endohedral fullerenes. *J. Nanosci. Nanotechnol.* **2021**, *21*, 2446–2459. [CrossRef]
33. Saunders, M.; Jiménez-Vázquez, H.A.; Cross, R.J.; Poreda, R.J. Stable compounds of helium and neon: He@C<sub>60</sub> and Ne@C<sub>60</sub>. *Science* **1993**, *259*, 1428–1430. [CrossRef] [PubMed]
34. Guha, S.; Nakamoto, K. Electronic structures and spectral properties of endohedral fullerenes. *Coord. Chem. Rev.* **2005**, *249*, 1111–1132. [CrossRef]
35. Levin, A.A.; Breslavskaya, N.N. Energy of compressed endoatoms and the energy capacity of small endohedral rare-gas fullerenes. *Russ. Chem. Bull.* **2005**, *54*, 1999–2002. [CrossRef]
36. Yan, H.; Yu, S.; Wang, X.; He, Y.; Huang, W.; Yang, M. Dipole polarizabilities of noble gas endohedral fullerenes. *Chem. Phys. Lett.* **2008**, *456*, 223–226. [CrossRef]
37. Sabirov, D.S.; Bulgakov, R.G. Polarizability exaltation of endofullerenes X@C<sub>n</sub> (*n* = 20, 24, 28, 36, 50, and 60; X is a noble gas atom). *JETP Lett.* **2010**, *92*, 662–665. [CrossRef]
38. Sabirov, D.S.; Tukhbatullina, A.A.; Bulgakov, R.G. Compression of methane endofullerene CH<sub>4</sub>@C<sub>60</sub> as a potential route to endohedral covalent fullerene derivatives: A DFT study. *Fuller. Nanotub. Carbon Nanostruct.* **2015**, *23*, 835–842. [CrossRef]
39. Zakirova, A.D.; Sabirov, D.S. Volume of the fullerene cages of endofullerenes and hydrogenated endofullerenes with encapsulated atoms of noble gases and nonadditivity of their polarizability. *Russ. J. Phys. Chem. A* **2020**, *94*, 963–971. [CrossRef]
40. Osuna, S.; Swart, M.; Sola, M. The reactivity of endohedral fullerenes. What can be learnt from computational studies? *Phys. Chem. Chem. Phys.* **2011**, *13*, 3585–3603. [CrossRef]
41. Ma, F.; Li, Z.-R.; Zhou, Z.-J.; Wu, D.; Li, Y.; Wang, Y.-F.; Li, Z.-S. Modulated nonlinear optical responses and charge transfer transition in endohedral fullerene dimers Na@C<sub>60</sub>C<sub>60</sub>@F with *n*-fold covalent bond (*n* = 1, 2, 5, and 6) and long range ion bond. *J. Phys. Chem. C* **2010**, *114*, 11242–11247. [CrossRef]
42. Cioslowski, J.; Fleischmann, E.D. Endohedral complexes: Atoms and ions inside the C<sub>60</sub> cage. *J. Chem. Phys.* **1991**, *94*, 3730. [CrossRef]
43. Tukhbatullina, A.A.; Zakirova, A.D.; Sabirov, D.S. The volume of the cage of endohedral complexes of the C<sub>60</sub> fullerene and halogenide-ions. *Vestn. Bashkir. Univ.* **2021**, *26*, 602–604. [CrossRef]
44. Sabirov, D.S.; Tukhbatullina, A.A.; Shepelevich, I.S. Molecular size and molecular structure: Discriminating their changes upon chemical reactions in terms of information entropy. *J. Mol. Graph. Model.* **2022**, *110*, 108052. [CrossRef] [PubMed]
45. Fowler, P.W.; Manolopoulos, D.E. *An Atlas of Fullerenes*; Clarendon Press: Oxford, UK, 1995; p. 392.
46. Schwerdtfeger, P.; Wirz, L.N.; Avery, J. The topology of fullerenes. *WIREs Comput. Mol. Sci.* **2015**, *5*, 96–145. [CrossRef]
47. Lu, X.; Chen, Z. Curved pi-conjugation, aromaticity, and the related chemistry of small fullerenes (<C<sub>60</sub>) and single-walled carbon nanotubes. *Chem. Rev.* **2005**, *105*, 3643–3696. [CrossRef]
48. Sabirov, D.S. From endohedral complexes to endohedral fullerene covalent derivatives: A density functional theory prognosis of chemical transformation of water endofullerene H<sub>2</sub>O@C<sub>60</sub> upon its compression. *J. Phys. Chem. C* **2013**, *117*, 1178–1182. [CrossRef]
49. Pizzagalli, L. First principles molecular dynamics calculations of the mechanical properties of endofullerenes containing noble gas atoms or small molecules. *Phys. Chem. Chem. Phys.* **2022**, *24*, 9449–9458. [CrossRef]
50. Zhang, J.; Bowles, F.L.; Bearden, D.W.; Keith Ray, W.; Fuhrer, T.; Ye, Y.; Dixon, C.; Harich, K.; Helm, R.F.; Olmstead, M.M.; et al. A missing link in the transformation from asymmetric to symmetric metallofullerene cages implies a top-down fullerene formation mechanism. *Nat. Chem.* **2013**, *5*, 880–885. [CrossRef]
51. Hashikawa, Y.; Murata, Y. Water-mediated thermal rearrangement of a cage-opened C<sub>60</sub> derivative. *ChemPlusChem* **2021**, *86*, 1559–1562. [CrossRef]
52. Ugi, I.; Gillespie, P. Representation of chemical systems and interconversions *bybe* matrices and their transformation properties. *Angew. Chem.* **1971**, *10*, 914–915. [CrossRef]
53. Sabirov, D.S. Information entropy of mixing molecules and its application to molecular ensembles and chemical reactions. *Comput. Theor. Chem.* **2020**, *1187*, 112933. [CrossRef]
54. Chemcraft. Available online: <http://www.chemcraftprog.com> (accessed on 28 July 2021).
55. Silant'ev, A.V. Energy spectrum and optical absorption spectrum of fullerene C<sub>24</sub> within the Hubbard model. *Phys. Solid State* **2020**, *62*, 542–554. [CrossRef]
56. Kaiser, K.; Scriven, L.M.; Schulz, F.; Gawel, P.; Gross, L.; Anderson, H.L. An sp-hybridized molecular carbon allotrope, cyclo[18]carbon. *Science* **2019**, *365*, 1299–1301. [CrossRef] [PubMed]
57. Osawa, E. Formation mechanism of C<sub>60</sub> under nonequilibrium and irreversible conditions—An annotation. *Fuller. Nanotub. Carbon Nanostruct.* **2012**, *20*, 299–309. [CrossRef]
58. Yang, H.; Mercado, B.Q.; Jin, H.; Wang, Z.; Jiang, A.; Liu, Z.; Beavers, C.M.; Olmstead, M.M.; Balch, A.L. Fullerenes without symmetry: Crystallographic characterization of C<sub>1</sub>(30)-C<sub>90</sub> and C<sub>1</sub>(32)-C<sub>90</sub>. *Chem. Commun.* **2011**, *47*, 2068–2070. [CrossRef]
59. Tamm, N.B.; Guan, R.; Yang, S.; Troyanov, S.I. New isolated-pentagon-rule isomers of fullerene C<sub>96</sub> captured as chloro derivatives. *Eur. J. Inorg. Chem.* **2020**, *2020*, 2092–2095. [CrossRef]
60. Yang, S.; Wang, S.; Troyanov, S.I. The most stable isomers of giant fullerenes C<sub>102</sub> and C<sub>104</sub> captured as chlorides, C<sub>102</sub>(603)C<sub>118/20</sub> and C<sub>104</sub>(234)C<sub>116/18/20/22</sub>. *Chem.–Eur. J.* **2014**, *20*, 6875–6878. [CrossRef]

61. Tamm, N.B.; Yang, S.; Wei, T.; Troyanov, S.I. Five isolated pentagon rule isomers of higher fullerene C<sub>94</sub> captured as chlorides and CF<sub>3</sub> derivatives: C<sub>94</sub>(34)C<sub>114</sub>, C<sub>94</sub>(61)C<sub>120</sub>, C<sub>94</sub>(133)C<sub>122</sub>, C<sub>94</sub>(42)(CF<sub>3</sub>)<sub>16</sub>, and C<sub>94</sub>(43)(CF<sub>3</sub>)<sub>18</sub>. *Inorg. Chem.* **2015**, *54*, 2494–2496. [[CrossRef](#)]
62. Sabirov, D.S.; Khursan, S.L.; Bulgakov, R.G. 1,3-Dipolar addition reactions to fullerenes: The role of the local curvature of carbon surface. *Russ. Chem. Bull.* **2008**, *57*, 2520–2525. [[CrossRef](#)]
63. Manna, D.; Ghanty, T.K. Theoretical prediction of icosahedral U@C<sub>20</sub> and analogous systems with high HOMO–LUMO gap. *J. Phys. Chem. C* **2012**, *11*, 16716–16725. [[CrossRef](#)]
64. Matsuo, Y.; Okada, H.; Ueno, H. History of Li@C<sub>60</sub>. In *Endohedral Lithium-Containing Fullerenes*; Springer: Singapore, 2017; pp. 15–23. [[CrossRef](#)]
65. Chandler, H.J.; Stefanou, M.; Campbell, E.E.B.; Schaub, R. Li@C<sub>60</sub> as a multi-state molecular switch. *Nat. Commun.* **2019**, *10*, 2283. [[CrossRef](#)] [[PubMed](#)]
66. García-Hernández, D.A.; Machado, A.; Cataldo, F. Hydrogenation of [Li@C<sub>60</sub>]PF<sub>6</sub>: A comparison with fulleranes derived from C<sub>60</sub>. *Fuller. Nanotub. Carbon Nanostruct.* **2022**. [[CrossRef](#)]
67. Sokolov, V.I. Fullerene C<sub>60</sub> as a ligand with variable hapticity. *Dokl. Akad. Nauk* **1992**, *326*, 647.
68. Soto, D.; Salcedo, R. Coordination modes and different hapticities for fullerene organometallic complexes. *Molecules* **2012**, *17*, 7151–7168. [[CrossRef](#)] [[PubMed](#)]
69. Sure, R.; Hansen, A.; Schwerdtfeger, P.; Grimme, S. Comprehensive theoretical study of all 1812 C<sub>60</sub> isomers. *Phys. Chem. Chem. Phys.* **2017**, *19*, 14296–14305. [[CrossRef](#)] [[PubMed](#)]
70. Sabirov, D.; Koledina, K. Classification of isentropic molecules in terms of Shannon entropy. *EPJ Web Conf.* **2020**, *244*, 01016. [[CrossRef](#)]
71. Zhang, R.; Murata, M.; Aharen, T.; Wakamiya, A.; Shimoaka, T.; Hasegawa, T.; Murata, Y. Synthesis of a distinct water dimer inside fullerene C<sub>70</sub>. *Nat. Chem.* **2016**, *8*, 435–441. [[CrossRef](#)] [[PubMed](#)]
72. Khong, A.; Jiménez-Vázquez, H.A.; Saunders, M.; Cross, R.J.; Laskin, J.; Peres, T.; Lifshitz, C.; Strongin, R.; Smith, A.B. An NMR Study of He<sub>2</sub> Inside C<sub>70</sub>. *J. Am. Chem. Soc.* **1998**, *120*, 6380–6383. [[CrossRef](#)]
73. Morinaka, Y.; Sato, S.; Wakamiya, A.; Nikawa, H.; Mizorogi, N.; Tanabe, F.; Murata, M.; Komatsu, K.; Furukawa, K.; Kato, T.; et al. X-ray observation of a helium atom and placing a nitrogen atom inside He@C<sub>60</sub> and He@C<sub>70</sub>. *Nat. Commun.* **2015**, *4*, 1554. [[CrossRef](#)]
74. Sabirov, D.S.; Tukhbatullina, A.A.; Bulgakov, R.G. Dependence of static polarizabilities of C<sub>60</sub>X<sub>n</sub> fullerene cycloadducts on the number of added groups X = CH<sub>2</sub> and NH (n = 1–30). *Comput. Theor. Chem.* **2021**, *993*, 113–117. [[CrossRef](#)]
75. Sabirov, D.S.; Terentyev, A.O.; Bulgakov, R.G. Counting the isomers and estimation of anisotropy of polarizability of the selected C<sub>60</sub> and C<sub>70</sub> bisadducts promising for organic solar cells. *J. Phys. Chem. A* **2015**, *119*, 10697–10705. [[CrossRef](#)]
76. Bertz, S.H. Complexity of synthetic reactions. The use of complexity indices to evaluate reactions, transforms and. *New J. Chem.* **2003**, *27*, 860–869. [[CrossRef](#)]
77. Parrondo, J.; Horowitz, J.; Sagawa, T. Thermodynamics of information. *Nat. Phys.* **2015**, *11*, 131–139. [[CrossRef](#)]
78. Sagawa, T.; Ueda, M. Minimal energy cost for thermodynamic information processing: Measurement and information erasure. *Phys. Rev. Lett.* **2011**, *102*, 250602. [[CrossRef](#)] [[PubMed](#)]
79. Davis, S.; González, D. Hamiltonian formalism and path entropy maximization. *J. Phys. A Math. Theor.* **2015**, *48*, 425003. [[CrossRef](#)]
80. Parker, M.C.; Jeynes, C. Fullerene stability by geometrical thermodynamics. *ChemistrySelect* **2020**, *5*, 5–14. [[CrossRef](#)]